

# Low temperature specific heat of 12442-type $\text{KCa}_2\text{Fe}_4\text{As}_4\text{F}_2$ single crystals

Teng Wang,<sup>1,2,3</sup> Jianan Chu,<sup>1,2,4</sup> Jiaxin Feng,<sup>1,2,4</sup> Lingling Wang,<sup>1</sup> Xuguang Xu,<sup>3</sup> Wei Li,<sup>5,6,\*</sup> Hai-Hu Wen,<sup>7</sup> Xiaosong Liu,<sup>1,2,3</sup> and Gang Mu<sup>1,2,4,†</sup>

<sup>1</sup>State Key Laboratory of Functional Materials for Informatics,  
Shanghai Institute of Microsystem and Information Technology,  
Chinese Academy of Sciences, Shanghai 200050, China

<sup>2</sup>CAS Center for Excellence in Superconducting Electronics(CENSE), Shanghai 200050, China

<sup>3</sup>School of Physical Science and Technology, ShanghaiTech University, Shanghai 201210, China

<sup>4</sup>University of Chinese Academy of Sciences, Beijing 100049, China

<sup>5</sup>State Key Laboratory of Surface Physics and Department of Physics, Fudan University, Shanghai 200433, China

<sup>6</sup>Collaborative Innovation Center of Advanced Microstructures, Nanjing 210093, China

<sup>7</sup>Center for Superconducting Physics and Materials,

National Laboratory of Solid State Microstructures and Department of Physics, Nanjing University, Nanjing 210093, China

Low-temperature specific heat (SH) is measured for the 12442-type  $\text{KCa}_2\text{Fe}_4\text{As}_4\text{F}_2$  single crystal under different magnetic fields. A clear SH jump with the height of  $\Delta C/T|_{T_c} = 130$  mJ/mol  $\text{K}^2$  is observed at the superconducting transition temperature  $T_c$ . It is found that the electronic SH coefficient  $\Delta\gamma(H)$  quickly increases when the field is in the low-field region below 3 T and then considerably slows down the increase with a further increase in the field, which indicates a rather strong anisotropy or multi-gap feature with a small minimum in the superconducting gap(s). The temperature-dependent SH data indicates the presence of the  $T^2$  term, which supplies further information and supports the picture with a line-nodal gap structure. Moreover, the onset point of the SH transition remains almost unchanged under the field as high as 9 T, which is similar to that observed in cuprates, and placed this system in the middle between the BCS limit and the Bose-Einstein condensation.

PACS numbers: 74.20.Rp, 74.70.Xa, 74.62.Dh, 65.40.Ba

## 1 Introduction

From the structural point of view, most Fe-based superconductors (FeSCs) belong to monolayered, e.g., 1111 and 21311 systems [1, 2], and infinite-layered systems, e.g., 11 and 122 systems [3, 4]. The only exception is the 12442 system [5–9], which has two FeAs layers between neighboring insulating layers. This new system has the general chemical formula of  $\text{AB}_2\text{Fe}_4\text{As}_4\text{C}_2$  ( $A = \text{K, Rb, and Cs}$ ;  $B = \text{Ca, Nd, Sm, Gd, Tb, Dy, and Ho}$ ;  $C = \text{F and O}$ ) and has attracted considerable research interest in recent years [10–21]. First principle calculations revealed a rather complicated band structure with ten Fermi surfaces (FSs) [10]. The superconducting (SC) transition temperature can be tuned by cobalt substitution [11]. Single crystals with the size of several millimeters were grown using the self-flux method [12, 13]. An abnormally high slope of the upper critical field vs.  $T_c$  and a rather strong Pauli paramagnetic effect have been also reported [13, 14]. The SC gap structure has been investigated by the muon spin relaxation ( $\mu\text{SR}$ ), heat transport, lower critical field, optical spectroscopy, and angle-resolved photoemission spectroscopy (ARPES) measurements [12, 15–19, 21]. However, the conclusions are rather controversial. The lower critical field study revealed a multi-gap feature with a clear difference in gap sizes [12]. The nodal gap structure has been indicated by  $\mu\text{SR}$  measurements [15–17]. Whereas the heat transport [18], optical spectroscopy [19], and recent

ARPES measurements [21] have supported a nodeless scenario. Even within the nodeless scenario, the estimation of the ratio between large and small gaps ( $\Delta_L/\Delta_S$ ) is also contradictory. On the basis of heat transport experiments [18], an estimation  $\Delta_L/\Delta_S \approx 2$  was proposed. The analysis of the lower critical field data [12] indicates that  $\Delta_L/\Delta_S \approx 2.9$ . ARPES measurements [21] provide an even larger value of  $\Delta_L/\Delta_S \approx 4$ . Consequently, more experiments by other techniques are urgently required to clarify this argument.

Specific heat (SH) is a bulk tool to detect the quasi-particle density of states (DOS) at the Fermi level, which can provide information about the gap structure [22–25]. The variation in electronic SH in SC states vs. temperature and field is rather different for different gap structures [26, 27], which can be used as a reliable criterion to probe the information of superconducting gap. Although the SH data have been shown in the previous studies [5, 18], an in-depth investigation is still lacking. In this study, we present an in-depth low temperature SH study of the 12442-type  $\text{KCa}_2\text{Fe}_4\text{As}_4\text{F}_2$  single crystal. A clear SH jump with the height of 130 mJ/mol  $\text{K}^2$  is observed. A quick increase in the electronic SH coefficient and the presence of the  $T^2$  term reveal a very large anisotropy with line nodes in the gap structure. Moreover, the feature of the SH anomaly around  $T_c$  under field diverges from the BCS picture and indicates an evolution tendency toward the Bose-Einstein condensation (BEC).

### 3 Results and discussion

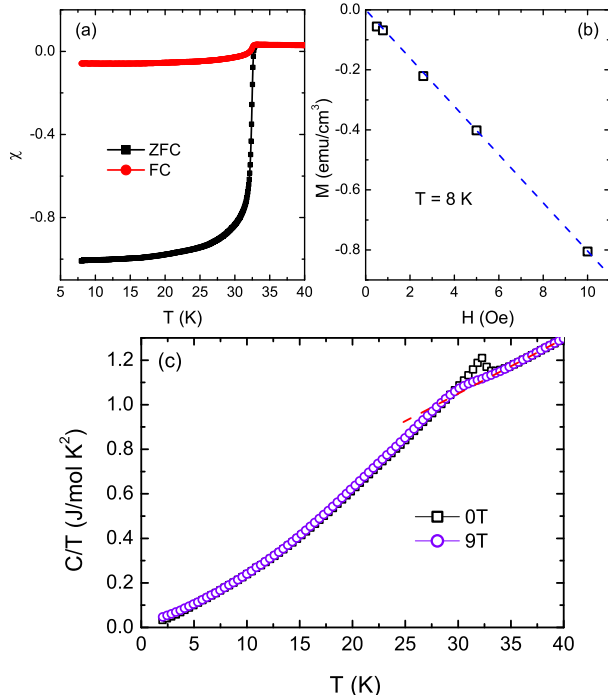


FIG. 1: (color online) (a) Temperature dependence of magnetic susceptibility for the  $\text{KCa}_2\text{Fe}_4\text{As}_4\text{F}_2$  single crystal. The applied magnetic field is 1 Oe. (b) Field dependence of magnetization at 8 K. The blue straight dashed line is a guide for the eye. (c) Temperature dependence of SH plotted as  $C/T$  vs.  $T$  under the two fields of 0 T and 9 T.

## 2 Materials and methods

$\text{KCa}_2\text{Fe}_4\text{As}_4\text{F}_2$  single crystals were grown by the self-flux method. The sample for the SH measurement has a mass of 2.3 mg. The detailed growth conditions and sample characterizations have been reported in our previous work [13]. The magnetic susceptibility measurements were performed with a superconducting quantum interference device (Quantum Design, MPMS 3). SH was measured on a physical property measurement system (Quantum Design, PPMS). Similar to that reported in our previous work [28], we employed the thermal relaxation technique to perform the SH measurements and the external field was applied along the  $c$  axis of the single crystal during the SH measurements.

The first principles calculations were performed using the all-electron full potential linear augmented plane wave plus local orbitals (FP-LAPW+lo) method [29], as implemented in the WIEN2K code [30]. The exchange-correlation potential was calculated using the generalized gradient approximation as proposed by Pedrew, Burke, and Ernzerhof [31]. Throughout the calculations, we fixed the crystal structure to the experimental values [5].

The superconducting transition of the single crystal was evaluated by magnetic susceptibility ( $\chi$ ) measurements. In Fig. 1(a), the  $\chi - T$  curve shows a clear and sharp SC transition at approximately 32.5 K, which indicates the high quality of the selected sample. The magnetic field was applied parallel to the  $ab$ -plane of the crystal to minimize the effect of demagnetization. To ensure the accurate calculation of superconducting volume fraction, we also measured the field dependence of magnetization, which is shown in Fig. 2(b). From this linear in-field behavior, the value of  $\chi$  was determined to be very close to  $-1$ , which indicated a high superconducting volume fraction of about 100% in our sample. Figure 1(c) shows the raw data for the SH coefficient  $\gamma = C/T$  vs.  $T$  at 0 T and 9 T. Here, one mole means the Avogadro number of the formula units (f.u.),  $\text{KCa}_2\text{Fe}_4\text{As}_4\text{F}_2$ . A clear and sharp SH anomaly owing to the SC transition can be seen near  $T_c$  from the raw data of 0 T. While for the data under 9 T, this anomaly becomes obscure. Within a limited temperature range above  $T_c$ ,  $C/T$  reveals a linear temperature dependence, as shown by the red dashed line in Fig. 1(c), which can be used as an estimation for the SH contribution of the normal states including the phonon term and the normal electronic term in this local temperature region in the vicinity of  $T_c$ .

Thus, we subtracted this linear straight line from the raw data, and the results are shown in Fig. 2(a). The SH anomaly  $\Delta C/T|_{T_c}$  at zero field was determined to be approximately 130 mJ/mol  $\text{K}^2$ , as indicated by the blue arrowed line. Of note, there are 4 Fe atoms in one formula unit of  $\text{KCa}_2\text{Fe}_4\text{As}_4\text{F}_2$ , which is twice that of 122 system, e.g.  $\text{Ba}_{0.6}\text{K}_{0.4}\text{Fe}_2\text{As}_2$ . Thus, the SH anomaly has to be reduced by half when compared with the 122 system, which amounts to 65 mJ/mol  $\text{K}^2$  for the 2-Fe-atoms case. Assuming a weak-coupling BCS picture with the ratio  $\Delta C/\gamma_n T|_{T_c} = 1.43$ , we can estimate the normal state electronic SH coefficient  $\gamma_n \approx 91$  mJ/mol  $\text{K}^2$ . For comparison with the theoretical prediction, we carried out first principles calculations; the results of electron DOS are shown in Fig. 2(b). The electronic SH data is related to the value of DOS at the Fermi level, which is  $N(E_F) = 4.75$   $\text{eV}^{-1}/\text{Fe}$  with both spins included. This value is quite consistent with the previous report on this material [10] and remarkably larger than that obtained in 1111 ( $\sim 2.62$   $\text{eV}^{-1}/\text{Fe}$ ) and 122 ( $\sim 2.3$   $\text{eV}^{-1}/\text{Fe}$ ) systems [32, 33]. By disregarding the coupling effects of electrons, the bare electronic SH coefficient  $\gamma_{bare}$  can be calculated using the formula [34]  $\gamma_{bare} = \pi^2 k_B^2 N(E_F)/3 = 11.2$  mJ/mol  $\text{K}^2$  (per mol Fe) = 44.8 mJ/mol  $\text{K}^2$  (per mol f.u.), where  $k_B$  is the Boltzmann constant. This bare value is approximately one half of the experimental result, which indicates a rather strong coupling of electrons in the real material.

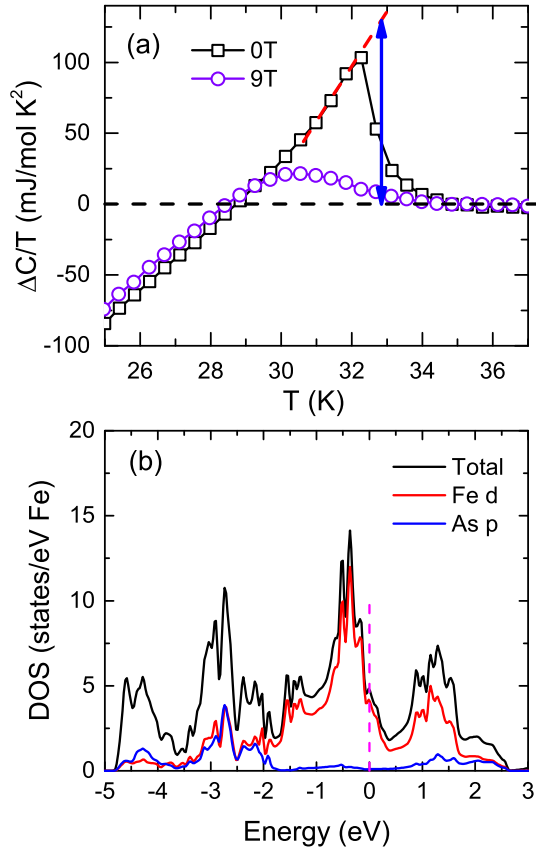


FIG. 2: (color online) (a) SH data after subtracting the linear background from the normal states. (b) Calculated electron DOS of  $\text{KCa}_2\text{Fe}_4\text{As}_4\text{F}_2$  plotted on a per Fe atom basis with both spins.

Next, we focus on the SH data in the low temperature range below 4.5 K, which is approximately  $1/7$  of  $T_c$ , to study low-energy excitations. Here, we plot the raw data of SH as  $C/T$  vs.  $T^2$  in Fig. 3(a). The data under different fields are shifted upwards by  $5 \text{ mJ/mol K}^2$  for clarity. No Schottky anomaly can be observed, which facilitates the following analysis of our data. As shown by the dotted violet line, all SH data under different fields reveal a tendency that slightly deviates from linear behavior, which cannot be simply described by

$$C(T, H) = \gamma(H)T + \beta T^3. \quad (1)$$

Here, the two terms are the normal electronic SH owing to the low-energy excitations by magnetic field and the phonon SH. Similar behaviors were reported in overdoped  $\text{Ba}(\text{Fe}_{1-x}\text{Co}_x)_2\text{As}_2$  and  $\text{Ba}(\text{Fe}_{1-x}\text{Ni}_x)_2\text{As}_2$  systems [25, 35]. To effectively simulate the negative curvatures of the experimental data, a  $T^2$  term should be considered in the electronic SH:

$$C(T, H) = \gamma(H)T + \alpha(H)T^2 + \beta T^3, \quad (2)$$

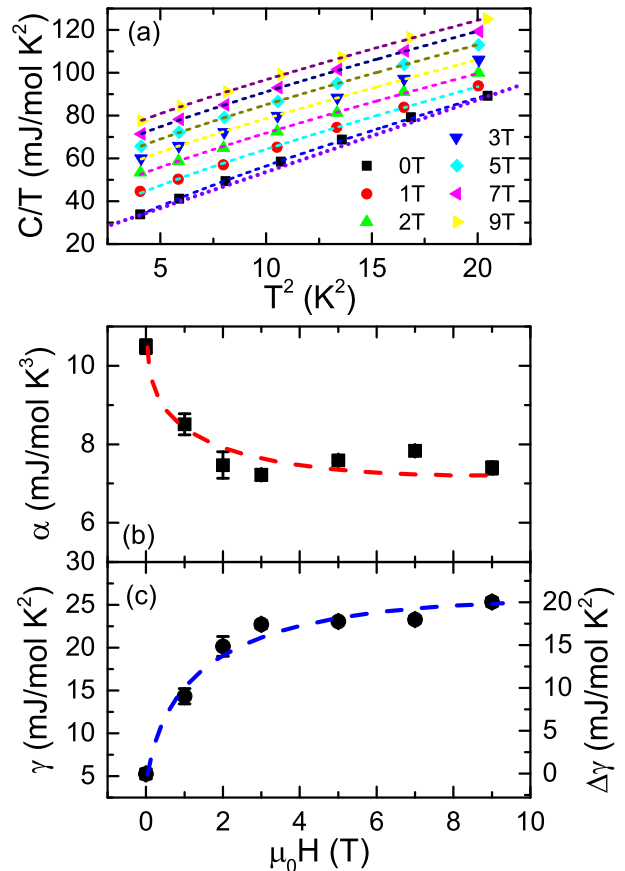


FIG. 3: (color online) (a) Raw data of SH under different fields in the low temperature region. The data are shown in the  $C/T$  vs.  $T^2$  plot. The data under different fields are shifted upwards by  $5 \text{ mJ/mol K}^2$  for clarity. The dashed lines are the results of theoretical fitting (see text). The dotted straight line is a guide for the eye. (b) and (c) Field dependence of the coefficient of the  $T^2$  term  $\alpha$  and the electronic SH coefficient  $\gamma$ . The dashed lines are the guide for the eye.

where  $\alpha(H)$  is the coefficient of the  $T^2$  term under the field  $H$ . To obtain reasonable results, during the fitting process, the values of  $\beta$  under fields are fixed to that of zero field ( $\sim 1.8 \text{ mJ/mol K}^4$ ). As shown by the dashed lines in Fig. 3(a), the fitting result is good. The presence of the  $T^2$  term in electronic SH is the hallmark of the line nodes in the energy gap(s) [26, 27]. The influence of the  $T^2$  term on the SH data is more significant at the lower temperatures. Thus, the confirmation by the lower-temperature experiments is needed in the future. Nevertheless, the obtained result indicates that line nodes are very likely to exist in the gap(s) of the 12442 system, which is consistent with the  $\mu\text{SR}$  measurements [15–17]. The results from the heat transport [18], optical spectroscopy [19], and ARPES [21] measurements support the nodeless picture. Thus, this issue requires more in-depth investigations in the future. Perhaps previous

studies on the Co-doped 122 system can be used as a reference. In the case of  $\text{Ba}(\text{Fe}_{1-x}\text{Co}_x)_2\text{As}_2$ , nodes can only be detected from the heat transport measurements when the heat current is parallel to the  $c$  axis of the crystal [36].

The fitting parameters  $\alpha(H)$  and  $\gamma$  are shown in Figs. 3(b) and (c). The value of  $\alpha(H)$  shows a clear decrease with an increase in the magnetic field up to 9 T, which is similar to that observed in the overdoped 122 system [25, 35]. Under zero field, a residual term  $\gamma_0 \equiv \gamma(0) \approx 5.3 \text{ mJ/mol K}^2$  was revealed. Because there are 4 Fe in one f.u., this value is comparable to that of the 122 system [24, 37]. Typically, this term is attributed to the non-superconducting fraction of the sample [28] and/or the residual quasiparticle DOS in the SC materials with nodes or  $S^\pm$  gap symmetry [22, 37]. Because the SC volume fraction of approximately 100% was confirmed by the magnetization measurement, the former possible origin can be ruled out, and  $\gamma_0$  may originate from the residual quasiparticle DOS owing to the unconventional gap symmetry, especially the possible existence of line nodes, in the present system.

The field-induced term  $\Delta\gamma = \gamma(H) - \gamma_0$  reflects the information about the SC gap. It is difficult to describe the field dependence of  $\Delta\gamma$  using a simple formula owing to the multi-band effect in this system [10]. Nevertheless, qualitatively,  $\Delta\gamma$  increases more quickly in the system with a small minimum for the multi-gap case or with a highly anisotropic gap structure, as has been observed in  $\text{MgB}_2$  [38] and cuprates [22]. This is because considerable quasiparticle DOS can be induced by the magnetic field around the Fermi surface with the gap minimum. A quick increase in  $\gamma$  with the field below 3 T in our data, as shown in Fig. 3(c), reflects this situation. Considering the multi-band feature of this system [10], typically there are two possibilities: (i) a large anisotropy occurring on an individual FS sheet; (ii) a considerable difference in the gap amplitudes between different FS sheets, at least one of which is very small. Combined with the results that the  $T^2$  term was discovered in electronic SH, the former is the more likely scenario. Regarding the situation in the relatively high field region above 3 T, the slow crawl of  $\Delta\gamma$  with field indicates the possible presence of larger full gap(s) in some certain FSs, which is consistent with the multi-gap picture.

We noticed that the quick increase in  $\Delta\gamma$  is accompanied by the considerable suppression of the SH jump at approximately  $T_c$  under magnetic field. To have a vivid impression, we plot the SH data at approximately  $T_c$  of  $\text{Ba}_{0.6}\text{K}_{0.4}\text{Fe}_2\text{As}_2$  [24] and  $\text{KCa}_2\text{Fe}_4\text{As}_4\text{F}_2$  in Figs. 4(a) and (b) respectively, both of which are normalized to the position and height of the SH peak under zero field. For the case of  $\text{Ba}_{0.6}\text{K}_{0.4}\text{Fe}_2\text{As}_2$ , the field of 9 T only suppresses the SH jump by 36%. Up to 79% of the SH jump of  $\text{KCa}_2\text{Fe}_4\text{As}_4\text{F}_2$  was suppressed by the same field. This is a very large discrepancy between the two values. To have a more accurate comparison, we need to consider

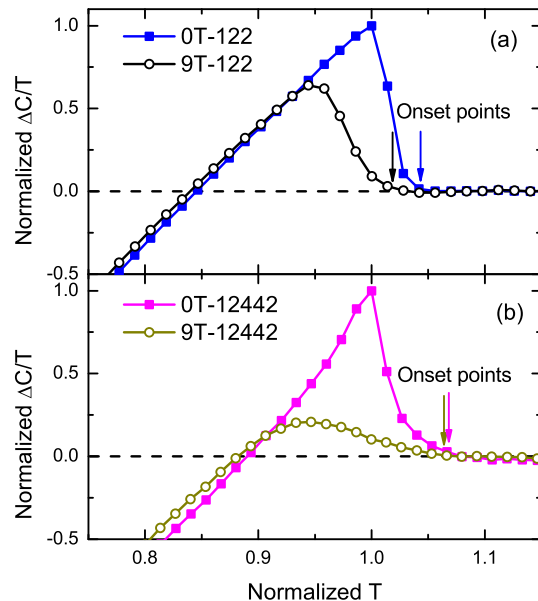


FIG. 4: (color online) SH data at the transition for  $\text{Ba}_{0.6}\text{K}_{0.4}\text{Fe}_2\text{As}_2$  (122, Ref. [24]) and  $\text{KCa}_2\text{Fe}_4\text{As}_4\text{F}_2$  (12442, this work). The scales of both coordinate axes are normalized.

the out-of-plane upper critical field  $H_{c2}^c$  of the two systems. The  $T_c$  (the slope of  $H_{c2}^c$  near  $T_c$ ,  $d\mu_0 H_{c2}^c/dT|_{T_c}$ ) of  $\text{Ba}_{0.6}\text{K}_{0.4}\text{Fe}_2\text{As}_2$  is slightly higher (lower) than that of  $\text{KCa}_2\text{Fe}_4\text{As}_4\text{F}_2$  [13, 24]. Assuming a similar evolution tendency for  $H_{c2}^c$  of the two materials toward lower temperature, the zero temperature value of  $H_{c2}^c(0)$  is slightly higher for  $\text{KCa}_2\text{Fe}_4\text{As}_4\text{F}_2$ . Thus, the more pronounced suppression of the SH jump in this 12442 system is not due to the difference in  $H_{c2}^c(0)$  and may be the reflection of the highly anisotropic SC gap(s).

Another notable feature is the almost unchanged onset point of the SH anomaly under 9 T compared with the zero field data [see the arrowed lines in Fig. 4(b)]. However, the transition temperature in resistivity data has been clearly suppressed by the out-of-plane field [13]. It is important because within the BCS picture, this onset point in SH should shift monotonously to lower temperature, just as that observed in conventional superconductors [23, 39]. Compared to the 122 system  $\text{Ba}_{0.6}\text{K}_{0.4}\text{Fe}_2\text{As}_2$  [see Fig. 4(a)], this feature is also noteworthy. Specifically, the field of 9 T suppresses the onset point by more than 0.4% for  $\text{KCa}_2\text{Fe}_4\text{As}_4\text{F}_2$ , while this value is as high as 2.4% for  $\text{Ba}_{0.6}\text{K}_{0.4}\text{Fe}_2\text{As}_2$ . This abnormal behavior has been reported in cuprates and has attracted considerable attention in the 1990s [40–42]. With the effort from both the experimental and theoretical sides, this was interpreted by a crossover from BCS-like superconductivity for weak coupling to BEC-like superconductivity for strong coupling [42]. The variable

that controls such crossover was identified as  $k_F\xi$  [43] and sometimes as  $\Delta/E_F$  for convenience [44], where  $k_F$  is the Fermi electron wave number,  $\xi$  is the coherence length,  $\Delta$  is the SC gap, and  $E_F$  is the Fermi energy. The unexpected high values of  $d\mu_0 H_{c2}^c/dT|_{T_c}$  and  $d\mu_0 H_{c2}^{ab}/dT|_{T_c}$  [13] may result in a small coherence length  $\xi$ . The recent ARPES results [21] have shown that the bottoms of the electronic-type bands barely touch the Fermi level and form a small electron-like elliptical Fermi pocket, which indicates the very small amplitude of  $k_F$  and  $E_F$ , although the detailed values were not provided. Meanwhile, the SC gap in the electronic-type  $\delta$  FS is as large as 5.3 meV. Thus, at least within the electronic FS, we can expect a small value of the parameter  $k_F\xi$  and a relatively large  $\Delta/E_F$ . We speculated that this is the internal reason for the departure from the BCS limit and tending to the BEC limit of this system. A more accurate estimation and analysis are needed in the future to further confirm our speculation.

#### 4 Conclusions

In summary, we studied the low-temperature SH of the 12442-type  $\text{KCa}_2\text{Fe}_4\text{As}_4\text{F}_2$  single crystal. We observed a clear SH jump with the height of 130 mJ/mol K. The electronic SH coefficient  $\Delta\gamma$  shows a fast increase with field in the low-field region below 3 T. Considering the presence of the  $T^2$  term in the SH data, the line nodal gap structure is a very large possibility in the 12442 system. This conclusion is further supported by the severe suppression of the SH jump by the magnetic field. Moreover, the onset point of the SH jump is not affected by the field, which is inconsistent with the BCS picture and locates the present system on the crossover from the BCS to BEC limit.

This work is supported by the Youth Innovation Promotion Association of the Chinese Academy of Sciences (No. 2015187), the Natural Science Foundation of China (No. 11204338), and the ‘‘Strategic Priority Research Program (B)’’ of the Chinese Academy of Sciences (No. XDB04040300). W.L. also acknowledges the start-up funding from Fudan University. The authors would like to thank Enago (www.enago.cn) for the English language review.

---

\* w'li@fudan.edu.cn

† mugang@mail.sim.ac.cn

- [1] Y. Kamihara, T. Watanabe, M. Hirano, and H. Hosono, *J. Am. Chem. Soc.* **130**, 3296 (2008).  
 [2] X. Zhu, F. Han, G. Mu, P. Cheng, B. Shen, B. Zeng, and H.-H. Wen, *Phys. Rev. B* **79**, 220512(R) (2009).  
 [3] F.-C. Hsu, J.-Y. Luo, K.-W. Yeh, T.-K. Chen, T.-W. Huang, P. M. Wu, Y.-C. Lee, Y.-L. Huang, Y.-Y. Chu,

- D.-C. Yan, et al., *Proc. Natl. Acad. Sci. USA* **105**, 14262 (2008).  
 [4] M. Rotter, M. Tegel, and D. Johrendt, *Phys. Rev. Lett.* **101**, 107006 (2008).  
 [5] Z.-C. Wang, C.-Y. He, S.-Q. Wu, Z.-T. Tang, Y. Liu, A. Ablimit, C.-M. Feng, and G.-H. Cao, *J. Am. Chem. Soc.* **138**, 7856 (2016).  
 [6] Z. Wang, C. He, Z. Tang, S. Wu, and G. Cao, *Sci. China Mater.* **60**, 83 (2017).  
 [7] Z.-C. Wang, C.-Y. He, S.-Q. Wu, Z.-T. Tang, Y. Liu, A. Ablimit, Q. Tao, C.-M. Feng, Z.-A. Xu, and G.-H. Cao, *J. Phys.: Condens. Mat.* **29**, 11LT01 (2017).  
 [8] Z.-C. Wang, C.-Y. He, S.-Q. Wu, Z.-T. Tang, Y. Liu, and G.-H. Cao, *Chem. Mater.* **29**, 1805 (2017).  
 [9] S.-Q. Wu, Z.-C. Wang, C.-Y. He, Z.-T. Tang, Y. Liu, and G.-H. Cao, *Phys. Rev. Materials* **1**, 044804 (2017).  
 [10] G. Wang, Z. Wang, and X. Shi, *Europhys. Lett.* **116**, 37003 (2016).  
 [11] J. Ishida, S. Iimura, and H. Hosono, *Phys. Rev. B* **96**, 174522 (2017).  
 [12] Z. C. Wang, Y. Liu, S. Q. Wu, Y. T. Shao, Z. Ren, and G. H. Cao, *Phys. Rev. B* **99**, 144501 (2019).  
 [13] T. Wang, J. N. Chu, H. Jin, J. X. Feng, L. L. Wang, Y. K. Song, C. Zhang, W. Li, Z. J. Li, T. Hu, et al., *J. Phys. Chem. C* **123**, 12925 (2019).  
 [14] T. Wang, C. Zhang, L. C. Xu, J. H. Wang, S. Jiang, Z. W. Zhu, Z. S. Wang, J. N. Chu, J. X. Feng, L. L. Wang, et al., *Sci. China-Phys. Mech. Astron.* **63**, 227412 (2020).  
 [15] F. K. K. Kirschner, D. T. Adroja, Z.-C. Wang, F. Lang, M. Smidman, P. J. Baker, G.-H. Cao, and S. J. Blundell, *Phys. Rev. B* **97**, 060506(R) (2018).  
 [16] D. T. Adroja, F. K. K. Kirschner, F. Lang, M. Smidman, A. D. Hillier, Z.-C. Wang, G.-H. Cao, G. B. G. Stenning, and S. J. Blundell, *J. Phys. Soc. Jpn.* **87**, 124705 (2018).  
 [17] M. Smidman, F. K. K. Kirschner, D. T. Adroja, A. D. Hillier, F. Lang, Z. C. Wang, G. H. Cao, and S. J. Blundell, *Phys. Rev. B* **97**, 060509 (2018).  
 [18] Y. Y. Huang, Z. C. Wang, Y. J. Yu, J. M. Ni, Q. Li, E. J. Cheng, G. H. Cao, and S. Y. Li, *Phys. Rev. B* **99**, 020502(R) (2019).  
 [19] B. Xu, Z. C. Wang, E. Sheveleva, F. Lyzwa, P. Marsik, G. H. Cao, and C. Bernhard, *Phys. Rev. B* **99**, 125119 (2019).  
 [20] A. B. Yu, T. Wang, Y. F. Wu, Z. Huang, H. Xiao, G. Mu, and T. Hu, *Phys. Rev. B* **100**, 144505 (2019).  
 [21] D. Wu, W. Hong, C. Dong, X. Wu, Q. Sui, J. Huang, Q. Gao, C. Li, C. Song, H. Luo, et al., arXiv: p. 2001.04082 (2020).  
 [22] H.-H. Wen, Z.-Y. Liu, F. Zhou, J. Xiong, W. Ti, T. Xiang, S. Komiya, X. Sun, and Y. Ando, *Phys. Rev. B* **70**, 214505 (2004).  
 [23] G. Mu, Y. Wang, L. Shan, and H.-H. Wen, *Phys. Rev. B* **76**, 064527 (2007).  
 [24] G. Mu, H. Luo, Z. Wang, L. Shan, C. Ren, and H.-H. Wen, *Phys. Rev. B* **79**, 174501 (2009).  
 [25] G. Mu, J. Tang, Y. Tanabe, J. Xu, S. Heguri, and K. Tanigaki, *Phys. Rev. B* **84**, 054505 (2011).  
 [26] M. Sigrist and K. Ueda, *Rev. Mod. Phys.* **63**, 239 (1991).  
 [27] N. E. Hussey, *Adv. Phys.* **51**, 1685 (2002).  
 [28] J. N. Chu, T. Wang, Y. H. Ma, J. X. Feng, L. L. Wang, X. G. Xu, W. Li, G. Mu, and X. M. Xie, *J. Phys.: Condens. Matter* **31**, 455602 (2019).  
 [29] D. J. Singh and L. Nordstrom, *Planewaves, Pseudopotentials*

- tials, and the LAPW Method* (Springer-Verlag, Berlin, 2006).
- [30] P. Blaha, K. Schwarz, G. Madsen, D. Kvasnicka, and J. Luitz, *An Augmented PlaneWave + Local Orbitals Program for Calculating Crystal Properties* (Technical Univiersity Wien, Austria, 2001).
- [31] J. P. Perdew, K. Burke, and M. Ernzerhof, Phys. Rev. Lett. **77**, 3865 (1996).
- [32] D. J. Singh and M.-H. Du, Phys. Rev. Lett. **100**, 237003 (2008).
- [33] D. J. Singh, Phys. Rev. B **78**, 094511 (2008).
- [34] A. Tari, *The Specific Heat of Matter at Low Temperatures* (Imperial College Press, 2003).
- [35] G. Mu, B. Gao, X. X. Xie, Y. Tanabe, J. Xu, J. Wu, and K. Tanigaki, Adv. Cond. Matter Phys. **2015**, 419017 (2015).
- [36] J.-P. Reid, M. A. Tanatar, X. G. Luo, H. Shakeripour, N. Doiron-Leyraud, N. Ni, S. L. Bud'ko, P. C. Canfield, R. Prozorov, and L. Taillefer, Phys. Rev. B **82**, 064501 (2010).
- [37] G. Mu, B. Zeng, P. Cheng, Z.-S. Wang, L. Fang, B. Shen, L. Shan, C. Ren, and H.-H. Wen, Chin. Phys. Lett. **27**, 037402 (2010).
- [38] F. Bouquet, R. A. Fisher, N. E. Phillips, D. G. Hinks, and J. D. Jorgensen, Phys. Rev. Lett. **87**, 047001 (2001).
- [39] H.-H. Wen, G. Mu, H. Luo, H. Yang, L. Shan, C. Ren, P. Cheng, J. Yan, and L. Fang, Phys. Rev. Lett. **103**, 067002 (2009).
- [40] A. Junod, K.-Q. Wang, T. Tsukamoto, G. Triscone, B. Revaz, E. Walker, and J. Muller, Physica C: Superconductivity **229**, 209 (1994).
- [41] A. S. Alexandrov, W. H. Beere, V. V. Kabanov, and W. Y. Liang, Phys. Rev. Lett. **79**, 1551 (1997).
- [42] A. Junod, A. Erb, and C. Renner, Physica C: Superconductivity **317-318**, 333 (1999).
- [43] F. Pistolesi and G. C. Strinati, Phys. Rev. B **49**, 6356 (1994).
- [44] S. Kasahara, T. Watashige, T. Hanaguri, Y. Kohsaka, T. Yamashita, Y. Shimoyama, Y. Mizukami, R. Endo, H. Ikeda, K. Aoyama, et al., Proc. Nat. Acad. Sci. USA **111**, 16309 (2014).